Preformed Seeds Modulate Native Insulin Aggregation Kinetics

ARTICLE *in* THE JOURNAL OF PHYSICAL CHEMISTRY B · NOVEMBER 2015

Impact Factor: 3.3 · DOI: 10.1021/acs.jpcb.5b07221

5 AUTHORS, INCLUDING:

Colina Dutta

Michigan Technological University

3 PUBLICATIONS **29** CITATIONS

SEE PROFILE

Mu Yang

Michigan Technological University

4 PUBLICATIONS **11** CITATIONS

SEE PROFILE

Fei Long

Michigan Technological University

7 PUBLICATIONS **6** CITATIONS

SEE PROFILE

THE JOURNAL OF PHYSICAL CHEMISTRY B

Article

pubs.acs.org/JPCB

Preformed Seeds Modulate Native Insulin Aggregation Kinetics

Colina Dutta,[†] Mu Yang,[†] Fei Long,[‡] Reza Shahbazian-Yassar,[‡,§] and Ashutosh Tiwari*[,†]

[†]Department of Chemistry, Michigan Technological University, Houghton, Michigan 49931, United States

[‡]Department of Mechanical Engineering, Michigan Technological University, Houghton, Michigan 49931, United States

[§]Department of Mechanical and Industrial Engineering, University of Illinois at Chicago, Chicago, Illinois 60607, United States

Supporting Information

ABSTRACT: Insulin aggregates under storage conditions via disulfide interchange reaction. It is also known to form aggregates at the site of repeated injections in diabetes patients, leading to injection amyloidosis. This has fueled research in pharmaceutical and biotechnology industry as well as in academia to understand factors that modulate insulin stability and aggregation. The main aim of this study is to understand the factors that modulate aggregation propensity of insulin under conditions close to physiological and measure effect of "*seeds*" on aggregation kinetics. We explored the aggregation kinetics of insulin at pH 7.2 and 37 °C in the presence of disulfide-reducing agent dithiothreitol (DTT), using spectroscopy (UV−visible, fluorescence, and Fourier transform infrared spectroscopy) and microscopy (scanning electron microscopy, atomic force microscopy) techniques. We prepared insulin "*seeds*" by incubating disulfide-reduced insulin at pH 7.2 and 37 °C for varying lengths of time (10 min to 12 h). These seeds were added to the native protein and nucleation-dependent aggregation kinetics was measured. Aggregation kinetics was fastest in the presence of 10 min seeds suggesting they were *nascent*. Interestingly, *intermediate* seeds (30 min to 4 h incubation) resulted in formation of transient fibrils in 4 h that converted to amorphous aggregates upon longer incubation of 24 h. Overall, the results show that insulin under disulfide reducing conditions at pH and temperature close to physiological favors amorphous aggregate formation and seed "maturity" plays an important role in nucleation dependent aggregation kinetics.

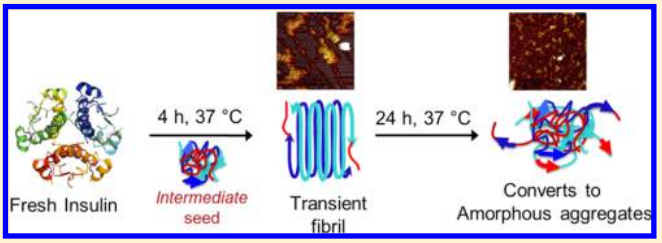

INTRODUCTION

More than 29 million people have diabetes in USA alone and this number is on the rise with more than one million new cases of diabetes diagnosed every year.[1] Nearly 14% of these patients take insulin, a globular hormone that has been used as treatment of insulin-dependent diabetes for more than seven decades.[1] Studies in the last two decades show that insulin plays an important role in cognition and memory. Insulin is also known to regulate metabolism of β-amyloid peptide and phosphorylation of τ-protein that is robustly linked to Alzheimer's disease.[2] Even though, insulin has been used for diabetes for several decades, its high cost due to poor stability and ease of forming aggregates when stored is a major challenge for the pharmaceutical industry. Insulin undergoes self-association by disulfide interchange reaction and aggregates under storage conditions.[3,4] Previous works show that insulin tends to precipitate when reacted with a disulfide interchange enzyme in the presence of reducing agent. This aggregation was attributed to scrambling of disulfide bonds.[5,6] In addition, insulin can also aggregate at the site of injection in the subcutaneous tissue which has a pH of ~7.2.[7,8] Even though, several insulin aggregation studies have been carried out at neutral pH either at high temperature or in the presence of chaotropic agents (e.g., urea or guanidine hydrochloride),[9,10] very few studies have explored insulin aggregation under conditions close to physiological.[11−13] Therefore, it is important to understand the factors that govern insulin stability and aggregation at neutral pH at which insulin is generally stored. Understanding the mechanism of insulin denaturation and aggregation during storage conditions will help in formulating effective solutions to increase the shelf life of the protein and prevent injection amyloidosis.

Insulin consists of two polypeptide chains: a 21-residue A-chain and a 30-residue B-chain. It has 3 disulfide bridges that stabilize the protein structure; two interchain disulfide bonds (A7−B7, A20−B19) and one intra-A-chain (A6−A11) disulfide bond.[14,15] At acidic conditions, insulin is predominantly a monomer and the hexamer prevails at neutral pH[16] (Figure 1). Insulin fibrils have been reported in case of human insulinoma as well as in pancreatic tumors.[17] Classically, the aggregation propensity of this protein has been studied at acidic pH and elevated temperatures.[18−21] Under these conditions, it has been shown to form fibrils that exhibit characteristic amyloid properties that are assumed to start from partially unfolded monomeric intermediates.[22,23] Changes in pH, ionic strength, anions, and stabilizers affect the lag time and fibril growth formation in insulin suggesting the importance of hydrophobic and electrostatic interactions during initial aggregation

Received: July 25, 2015
Revised: October 30, 2015

DOI: 10.1021/acs.jpcb.5b07221
J. Phys. Chem. B XXXX, XXX, XXX−XXX

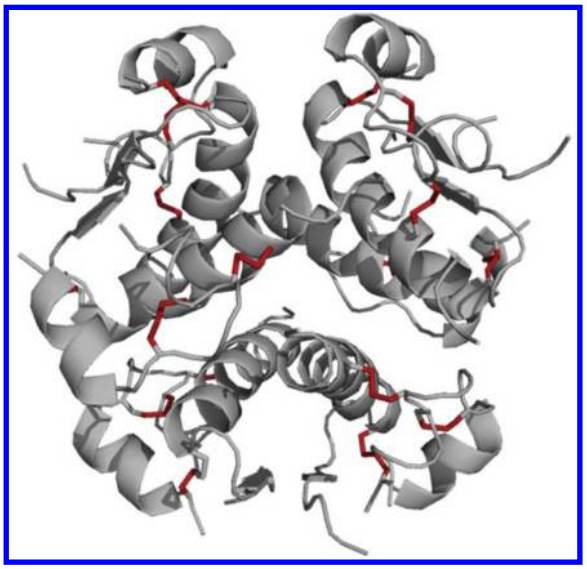

Figure 1. Ribbon structure of insulin hexamer at neutral pH. Firebrick red sticks are used to denote the disulfide bonds (−S−S−) between A7−B7, A20−B19, and A6−A11 positions in each monomer. The backbone is shown in gray color. The structures were generated using PyMOL 1.3 and PDB file 1AI0.[29]

process.[13] Studies involving solvation effects on insulin fibrillation exhibited aggregation in the presence of ethanol and trifluoroethanol.[22] All these studies point toward a general hypothesis that any external perturbation contributes toward insulin aggregation.[18,20,23−27]

Liquid insulin formulations prepared for diabetics, come with an expiration time span of 18−24 months. This long-term storage of insulin can lead to instability of the protein resulting in formation of unwanted products and possible complications such as injection amyloidosis when administered to patients.[14] One of the major cause of loss of native protein structure and aggregation is loss of critical S−S bonds or formation of scrambled disulfide bonds that destabilize the protein structure.[26,27] Previous studies on insulin with reduced and alkylated disulfide bonds showed increased aggregation rate when compared to insulin with intact disulfide bonds.[27,28] This underscores the importance of disulfide bonds in the overall stability and activity of the protein. Therefore, it is important to study how reducing environment near physiological pH can affect protein stability and hence modulate its aggregation over a period of time. In this study we show reduction of disulfide bonds of insulin leads to rapid aggregation within 10 min. Interestingly, we did not observe any fibrillar aggregates under these conditions. Instead, we observed amorphous insulin aggregates that stayed amorphous even after 6 months of incubation time. AFM images of native insulin in the presence of 30 min to 1 h insulin seeds show fibrillar aggregates after 4 h of incubation that converts to amorphous aggregates upon incubation for 24 h. Native insulin incubated with 10 min seeds form amorphous aggregates only. This study provides a mechanistic insight into insulin instability and how seeds from different stages of protein aggregation can affect native protein's aggregation kinetics and the nature of aggregates. This may help us better understand nucleation dependent aggregation process at the molecular level for improperly stored insulin and injection amyloidosis in diabetes patients.

MATERIALS AND METHODS

Unless otherwise indicated, all materials were used as supplied by the manufacturer without any further purification. Human recombinant insulin, dithiothreitol (DTT), thioflavin T (ThT), 8-anilino-1-naphthalenesulfonic acid (ANS) dye, and 4,4′-Dianilino-1,1′-binaphthyl-5,5′- disulfonic acid (bis-ANS) dye were purchased from Sigma.

Preparation of Insulin Samples. Insulin was dissolved in 0.025 M HCl at a concentration of 10 mg/mL. The protein was allowed to equilibrate overnight at 4 °C with mild agitation. To the insulin solution 0.025 M NaOH was added to neutralize the HCl. Then, insulin aliquots were made to the final concentration of 1 mg/mL (unless otherwise indicated) in 20 mM sodium phosphate buffer at pH 7.2 having 150 mM NaCl. All samples were prepared either in presence or absence of 10 mM dithiothreitol (DTT). The samples were prepared on ice followed by incubation at 37 °C for the indicated time periods (see figures for details). Blanks (contained everything except protein) were similarly prepared and incubated as samples and were used for background subtraction.

Seeding Activity of Disulfide-Reduced Insulin Aggregates. Insulin seeds were prepared by incubating 1 mg/mL (172 μM) insulin in the presence of 10 mM DTT in phosphate buffer, for 10 min, 30 min to 4 h (30 min intervals), and 4 to 12 h (1 h intervals) at 37 °C. Post incubation, seeds were washed with distilled water using Millipore Amicon Ultra centrifugal filters (3000 Da cutoff) and were added to freshly prepared native insulin sample (all disulfide bonds intact) at a concentration of 5%, 15% and 45% v/v. Negative controls were prepared using identical conditions as samples but in the absence of seeds. All samples were prepared on ice and then incubated at 37 °C for the indicated time. In addition to incubating insulin at 1 mg/mL (172 μM), samples were also diluted to a final protein concentration of 90 μM and 20 μM in phosphate buffer to study the effect of dilution on aggregation kinetics. All measurements were done in triplicates at 25 °C.

Matrix Assisted Laser Desorption/Ionization Time of Flight Mass Spectrometry (MALDI−TOF MS). Microflex LRF MALDI−TOF mass spectrometer (Bruker) equipped with microScout Ion Source was used to characterize disulfide states in the insulin samples. Insulin was incubated with 10 mM DTT for 0, 15 min, and 4 h at 37 °C. Fresh native insulin was used as control. Post incubation, samples (and control) were incubated with freshly prepared 100 mM iodoacetamide (IAA) for 2 h at room temperature to block the free sulfhydryl groups. Low molecular weight contaminants were removed using C_{18} ZipTip. Samples were prepared on the target using the direct droplet method. In this method, a saturated matrix solution of α-Cyano-4-Hydroxycinnamic acid was mixed with solvent (0.1% trifluoroacetic acid (TFA) with 33% acetonitrile (ACN)) having sample in 1:1 ratio v/v (matrix:solvent). From this mixture 1 μL of sample was aliquoted and dried at room temperature on the target before analyzing.

UV−Visible Absorbance Spectroscopy. Absorbance measurements were performed using a PerkinElmer Lambda 35 UV−visible spectrophotometer. After completion of incubation, absorbance of samples was measured at 600 nm in order to assess turbidity of insulin samples due to aggregation. All measurements were done at room temperature and in triplicates.

Intrinsic and Extrinsic Fluorescence. Fluorescence measurements were carried out using a Horiba Jobin Yvon

DOI: 10.1021/acs.jpcb.5b07221
J. Phys. Chem. B XXXX, XXX, XXX−XXX

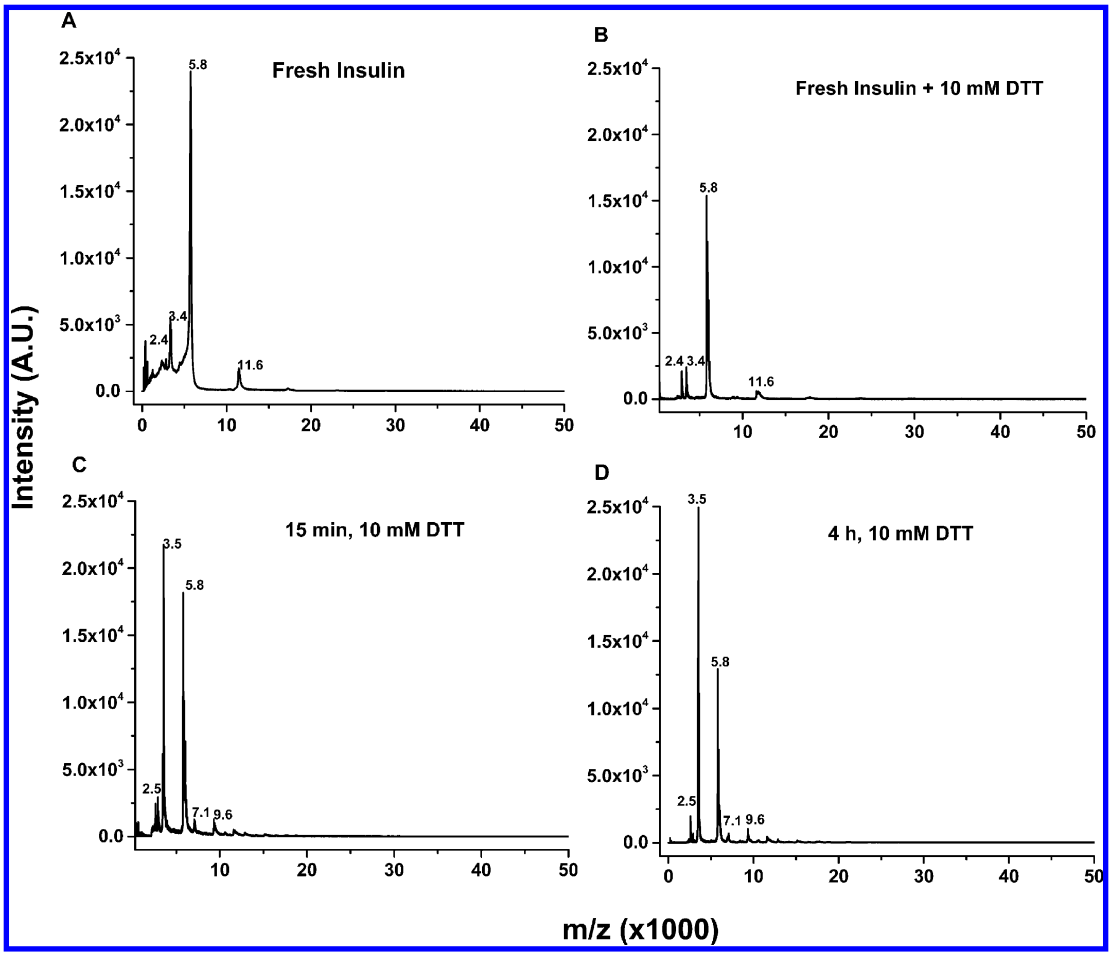

Figure 2. Mass spectrometry (MALDI–TOF) analysis showing effect of 10 mM DTT on disulfide status of insulin. Insulin was incubated with 10 mM DTT for 0 min, 15 min, and 4 h at 37 °C. Fresh insulin was used as control. Post incubation, samples (and control) were alkylated with 100 mM IAA for 2 h before running on MALDI–TOF. Fresh insulin in the presence and absence of reducing agents were similarly alkylated using IAA and were run as controls.

spectrofluorometer (Fluoromax-4). Excitation and emission slit widths were set at 2 nm, each. For intrinsic fluorescence, emission spectra were acquired from 285 to 450 nm with excitation at 280 nm. For extrinsic fluorescence, emission spectra were acquired in the presence of 10 μM ThT, 10 μM ANS, or 1 μM bis-ANS. The concentrations of dye stocks were determined using their extinction coefficients: ANS $\varepsilon_{350\ nm}$ = 5000 M^{-1} cm^{-1}, bis-ANS $\varepsilon_{385\ nm}$ = 16790 M^{-1} cm^{-1}, and ThT $\varepsilon_{416\ nm}$ = 26,620 M^{-1} cm^{-1}. Protein samples were equilibrated with respective fluorophores on ice, in dark for 30 min before acquiring the spectra. For ThT fluorescence, emission spectra were collected from 460 to 650 nm with excitation at 450 nm. Fluorescence spectra from 400 to 700 nm were collected with excitation at 380 nm for ANS and at 360 nm for bis-ANS. All measurements were done in triplicates.

Field Emission Scanning Electron Microscopy (FESEM). Electron microscope images were collected using Hitachi S-4700 field-emission scanning electron microscope (FESEM). Samples incubated for indicated times were diluted with double-distilled water and aliquoted in Millipore Amicon Ultra centrifugal filters (3000 Da cut off). The diluted samples were centrifuged at 7000 × *g* at 4 °C (three repeats after dilution with water) to remove low molecular weight impurities (salt, buffer etc.). The washed samples were aliquoted on SEM stubs and air-dried. The samples were platinum coated using a sputter coater and imaged using an acceleration voltage of 10 kV.

Atomic Force Microscopy (AFM). Aggregates of insulin were analyzed by aliquoting 7 μL of sample on a freshly cleaved mica surface at 25 °C. AFM imaging was performed on Dimension ICON AFM system (Bruker, CA, USA) using Peakforce Tapping mode. Scan-Asyst-Air cantilevers (Bruker, CA, USA) with spring constant 0.4 N/m and resonant frequency 70 kHz were selected as recommended by the manufacturer. AFM image analysis was carried out using NanoScope Analysis software from Bruker, CA, USA.

Nanomechanical measurements were performed using Dimension ICON AFM (Bruker, USA) under ambient conditions using Peakforce Tapping mode. RTESPA cantilevers (Bruker, USA) were selected with calibrated spring constant and tip radius of 55.6 N/m and 12 nm, respectively. For nanomechanical measurements, 1 mg/mL insulin was incubated with 45% v/v seeds (10 min, 30 min, 1 h, 4 h) for 4 h. Samples were prepared on freshly cleaved mica similar to AFM imaging. Derjaguin-Mueller–Toporov (DMT) modulus analysis was carried out using NanoScope software from Bruker, CA, USA. The Young's modulus value for each sample was calculated by averaging the moduli of each aggregate in a sample using the Nanoscope software.

DOI: 10.1021/acs.jpcb.5b07221
J. Phys. Chem. B XXXX, XXX, XXX–XXX

Fourier Transform-Infrared Spectroscopy (FT-IR). Secondary structure determination of insulin seeds were performed using PerkinElmer Frontier FT-IR spectrometer. *Seeds* were prepared by incubating 1 mg/mL insulin with 10 mM DTT at 37 °C for 10 min, 30 min, 1 and 4 h followed by washing as discussed earlier. A drop of sample was placed on the crystal and allowed to dry at room temperature. Data was acquired at a resolution of 4 cm^{-1} and 128 scans were averaged per sample. Data was analyzed between 1800 and 1600 cm^{-1} after subtracting the background. Raw spectra were deconvoluted using Gaussian model to obtain the component peaks and the contribution from each peaks was calculated by integrating area under the curves using Origin 9.1.

RESULTS

In this work, we monitored aggregation of insulin (Figure 1) in presence and absence of 10 mM DTT at pH 7.2 and at 37 °C. We also measured the aggregation kinetics of native insulin in the presence of "*seeds*" prepared by incubating disulfide-reduced insulin (insulin incubated with 10 mM DTT) for different time periods (10 min to 12 h). The kinetics, morphology, and secondary structure of the aggregates were studied using a variety of biophysical and analytical methods. Susceptibility of insulin to disulfide bond reduction was investigated using MALDI−TOF (Figure 2). Samples incubated for 15 min and 4 h with 10 mM DTT (Figure 2C, 2D) had the highest proportion of Insulin B-chain (3.5 kDa) along with dimers of full-length protein as well as B-chain (11.6 and 7.1 kDa respectively). Aggregated forms of B-chain dimer along with A-chain were also observed at a molecular mass of 9.6 kDa. Trace amounts of A-chain (2.5 kDa) and insulin monomer were also visible. Fresh insulin in the absence or presence of reducing agent predominantly showed the existence of intact insulin (Figure 2A, 2B). However, in the presence of 10 mM DTT, the interchain disulfide bonds in insulin were cleaved rapidly showing increase in B chain content (Figure 2C, 2D).

The extent of protein aggregation was monitored by measuring the turbidity (optical density (O.D.)) at 600 nm, using a UV−visible spectrophotometer (Figure 3). The absorbance of samples containing 10 mM DTT increased with increasing incubation time but was mostly unchanged for the control groups (proteins not treated with reducing agent). Significant increase in O.D. was observed within the first 1 h of incubation.

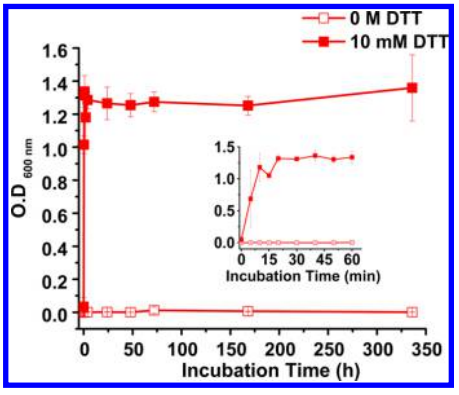

Figure 3. Protein aggregation monitored by UV absorbance. Insulin was incubated at 37 °C for the indicated time periods and UV absorbance of the samples were measured at 600 nm. Error bars indicate ± SD.

Insulin misfolding, conformational change, hydrophobic exposure, and aggregation were monitored by intrinsic and extrinsic fluorescence. Protein misfolding and conformational change for disulfide-reduced insulin was investigated by measuring the change in intrinsic fluorescence (Figure 4). We

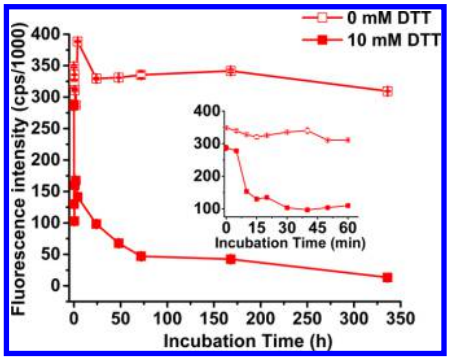

Figure 4. Insulin unfolding monitored by intrinsic fluorescence. Fluorescence spectra for 172 μM insulin incubated with/without 10 mM DTT were collected from 285 to 450 nm with excitation at 280 nm. Peak emission wavelength of 306 nm was selected. Peak fluorescence intensities are shown using open symbols (without DTT) and closed symbols (with 10 mM DTT). Inset shows a plot for the first 1 h of incubation. Error bars indicate ±SD.

used extrinsic fluorophores such as 8-anilino-1-naphthalene-sulfonic acid (ANS), to measure misfolding and extent of hydrophobic exposure; and 4,4′-Dianilino-1,1′-binaphthyl-5,5′-disulfonic acid (bis-ANS) as a conformational tightening agent and measure of hydrophobic exposure (Figure 5). Thioflavin T (ThT) was used to monitor the nature of aggregates (Figures 6 and 8). The morphology (Figures 7 and 9), and secondary structure (Figure 10) of the aggregates were further characterized by microscopy techniques (SEM, AFM) and FT-IR respectively.

Insulin samples incubated with 10 mM DTT show a rapid decline in fluorescence as a function of time, whereas no measurable change in fluorescence intensity was observed for the protein in the control groups (0 M DTT). The steepest drop in fluorescence intensity for DTT treated samples is observed in the first 20 min (inset in Figure 4). Fluorescence intensity continues to decrease rapidly up to 48 h and then slows down and the intensity stabilizes. Misfolding and hydrophobic exposure of insulin was monitored using ANS and bis-ANS (Figure 5). Both ANS and bis-ANS show a rapid increase in fluorescence intensity in the first 20 min and then was steady beyond 1 h of incubation time. Control samples (samples with no DTT) did not show any change in fluorescence upon addition of the dyes.

The nature and morphology of the aggregates were further characterized by ThT fluorescence, SEM and AFM imaging. ThT is known to bind to amyloid fibrils as well as large aggregates and fluoresces.[30,31] Fluorescence intensity for DTT treated insulin increased rapidly in the first 30 min of incubation, followed by a gradual increase upon longer incubation (Figure 6). Whereas, insulin incubated similarly but in absence of DTT (control groups) did not show any change in fluorescence intensity over the length of time. SEM images of insulin samples treated with DTT and incubated at 37 °C for different time periods (15 min, 2 h, 4 h, 168 h, or 6 months) were taken (Figures 7, S6 and S7). Freshly incubated insulin samples with and without DTT were imaged as controls

DOI: 10.1021/acs.jpcb.5b07221
J. Phys. Chem. B XXXX, XXX, XXX−XXX

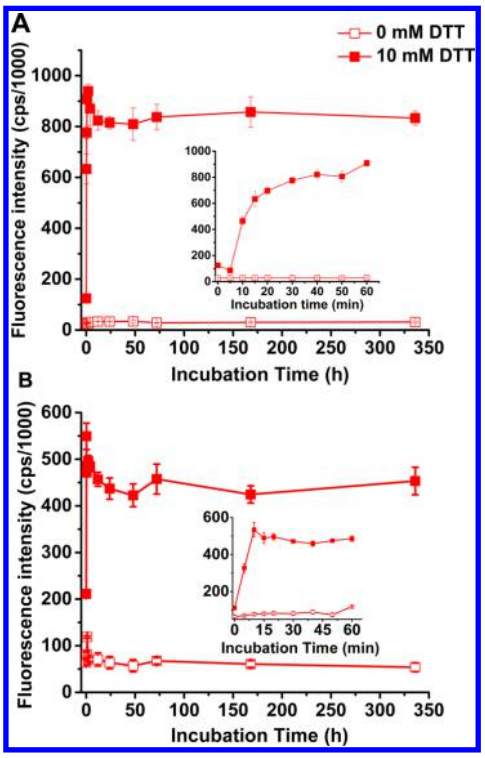

Figure 5. Protein misfolding and hydrophobic exposure monitored by ANS and bis-ANS fluorescence. Insulin samples at 172 μM concentration were incubated with 10 μM ANS or 1 μM bis-ANS for 15 min before acquiring spectra. Emission spectra were collected from 400 to 700 nm with excitation at 380 nm for (A) ANS and 360 nm for (B) bis-ANS. Average peak emission wavelengths of 467 and 482 nm were selected for ANS and bis-ANS, respectively. Peak fluorescence intensities are shown using open symbols (without DTT) and closed symbols (with 10 mM DTT). Inset shows a plot for the first 1 h of incubation. Error bars indicate ±SD.

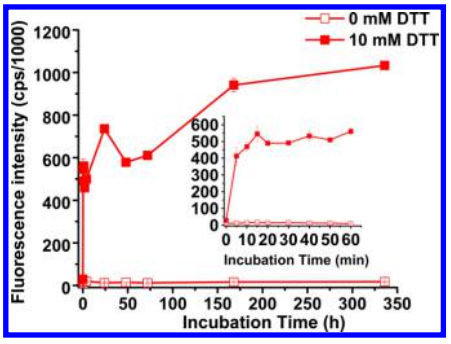

Figure 6. Protein aggregation monitored by ThT fluorescence. Emission spectra for 57 μM insulin in the presence of 10 μM ThT were acquired from 460 to 650 nm with excitation at 450 nm. Average emission peak wavelength of 486 nm was selected. Peak fluorescence intensities are shown using open symbols (without DTT) and closed symbols (with 10 mM DTT). Inset shows a plot for the first 1 h of incubation. Error bars indicate ±SD.

(Figure S6A, S6B). All the aggregates were amorphous in nature with an average subunit diameter of 200 ± 100 nm (Figure 7).[32] The morphology of aggregates remained unaltered even after a prolonged incubation of 6 months (Figure S7).

The effect of electrostatic interaction on insulin aggregation was studied in the absence as well as presence (150 or 300 mM) of NaCl. In addition, insulin concentration was also varied (20, 90, or 172 μM) (Figures S1−S3). Increasing the salt concentration up to 300 mM did not alter the overall aggregation kinetics (Figures S1−S3). Furthermore, change in insulin concentration (20, 90, or 172 μM) did not affect the overall trend for the fluorescence.

Seeding experiments were carried out by incubating native insulin with *seeds* for varying lengths of time at 37 °C. *Seeds* were prepared by incubating disulfide-reduced insulin at pH 7.2 at 37 °C for 10 min, 30 min to 4 h (30 min intervals) and 5 to 12 h (1 h intervals). Fresh insulin was incubated with 5%, 15%, and 45% v/v of various *seeds* prepared. The kinetics and morphology of insulin aggregates in the presence of seeds were analyzed by ThT fluorescence and AFM (Figures 8, 9, and S8−S14, Table S1). The aggregation kinetics of native insulin in the presence of *seeds* were calculated by fitting the ThT fluorescence data at 45% v/v seed concentration (Figure S14) until 4 h and the results are shown in Figure S13 and Table S1. Aggregation of native insulin was fastest in the presence of 10 min *seeds* (Figure S13, Table S1) followed by seeds incubated for 30 min and 1, 1.5, and 4 h. Seeds prepared by incubating insulin for longer time (5−12 h) showed a much slower aggregation kinetics. Control samples (fresh insulin incubated without seeds) did not show any change over the experiment period of 7 days. Since, 10 min *seeds* showed fast and extreme aggregation efficiency, effect of seed concentrations at 5%, 15%, and 45% v/v by ThT fluorescence on kinetics of native insulin aggregation was measured (Figure 8). Seed concentrations alter the aggregation kinetics with 5% *seeds* showing a gradual but continuous increase in fluorescence, 15% *seeds* showing a rapid initial increase in fluorescence followed by gradual increase in fluorescence, and 45% *seeds* showing a very rapid increase in fluorescence intensity that peaks by 4 h of incubation time and then stabilizes. Insulin aggregates were prepared in the presence of *seeds* (10 min, 30 min, 1 h, and 4 h) at a concentration of 45% v/v and were visualized using AFM with peak force tapping mode in air (Figures 9, S11, and S12). The elastic strength of the aggregates along the radial direction (Young's modulus) were measured using peak force QNM mode of AFM. This intrinsic stiffness of each aggregate in a sample was calculated using Nanoscope software and the average number was used to represent Young's moduli of aggregates generated using different timed *seeds*. The elastic strength of aggregates formed by incubating native insulin with different timed *seeds* (10 min, 30 min, 1 h, and 4 h) were comparable and ranged between 4 ± 0.6 and 6 ± 0.2 GPa. Aggregate population was maximum for protein incubated with 10 min *seeds* and it decreased with seed incubation time (Figure 9).

Secondary structure of the protein *seeds* (10 min, 30 min, 1 h, and 4 h) were analyzed using FT-IR (Figure 10) in the amide I band region (1700−1600 cm^{-1}). The raw spectra were deconvoluted using Gaussian model to obtain the component peaks. Native insulin showed a peak at 1656 cm^{-1} whereas seeds exhibited peaks at 1656 and 1625 cm^{-1} upon deconvolution. Area under the peaks were integrated to obtain the relative contribution of component peaks at 1656 and 1625 cm^{-1}, respectively.

DISCUSSION

Insulin can easily aggregate due to destabilizing influences and the nature and morphology of these aggregates are diverse.[11,18,19,33−35] Under extremes of conditions such as pH, temperature, or denaturants, insulin forms β-sheet rich

DOI: 10.1021/acs.jpcb.5b07221
J. Phys. Chem. B XXXX, XXX, XXX−XXX

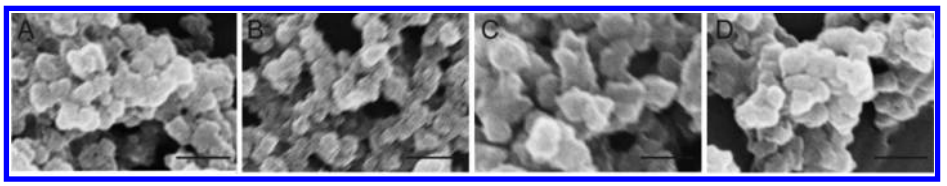

Figure 7. Scanning electron microscope images of insulin aggregates. Aggregates of insulin were imaged using SEM. Insulin samples were incubated at 37 °C with 10 mM DTT for (A) 15 min, (B) 2 h, (C) 4 h, and (D) 168 h, respectively. Scale bar for all panels is 500 nm.

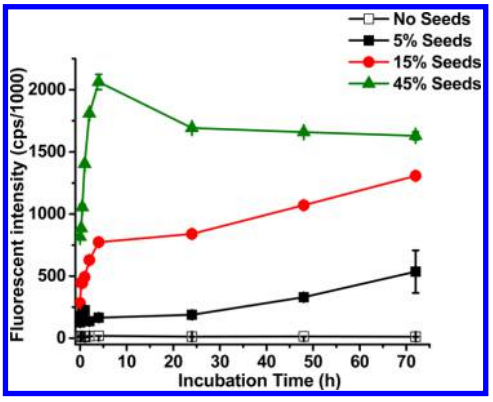

Figure 8. Effect of seeding concentration of *nascent* seeds on aggregation kinetics. *Nascent* Seeds prepared by incubating insulin with 10 mM DTT for 10 min were used at a concentration of 5%, 15%, and 45% v/v for seeding experiments. Protein aggregation was monitored by ThT fluorescence and was performed as detailed in Figure 6.

fibrils.[11,36] Several other aggregation studies at physiological pH and temperature in combination with external perturbations show that proteins can misfold and form a range of aggregate forms.[19,22,37] Both amyloid formation and amorphous aggregates have been reported in the disease process and have been shown to be dependent on external factors. In addition, importance of conserved disulfide bond providing stability to proteins has been explored in several studies.[38−40] It is known that insulin aggregates at storage conditions by a β-elimination reaction (scrambled disulfide bonds), and this may lead to aggregation of insulin at the injection site of diabetes patients leading to injection amyloidosis. Therefore, to better understand the kinetics and mechanism of insulin aggregation with compromised disulfide bonds; we studied the effect of different preformed *seeds* on the aggregation kinetics of native insulin. In this work, we used DTT as disulfide reducing agent to accelerate the disulfide scrambling process.

We measured the extent of disulfide reduction using MALDI−TOF mass spectrometry (Figure 2). Fresh insulin sample spectra showed that it was predominantly monomer (Figure 2A, 2B). Insulin incubated with 10 mM DTT for 15 min and 4 h show a significant increase in B-chain monomers (3.5 kDa) with appearance of a new peak at 7.1 kDa that indicates B-chain dimers. Relative abundance peak for insulin monomer (5.8 kDa) decreased in the presence of DTT when incubation time was increased from 15 min to 4 h. (Figure 2C, 2D). Appearance of a new peak was observed at 9.6 kDa for insulin incubated with DTT at 15 min and 4 h samples suggesting presence of aggregated forms of B-chain dimer with A-chain or presence of tetramer of A-chain. The data suggests cleavage of interchain disulfide bonds in insulin at positions A7-B7 and A20-B19 leading to generation of insulin A and B chains. An increase in molecular weight of ∼20−30 Da for the samples could be due to the residual buffer ions present as contaminants in the sample.

We monitored aggregation kinetics and secondary structure of insulin at pH 7.2, 37 °C using various spectroscopic techniques (Figures 2−6, 8 and 10) and morphology of aggregates were characterized by SEM and AFM (Figures 7 and 9).

We investigated the effect of 10 mM DTT on insulin instability and aggregation. As turbidity is a direct measure of the amount of aggregation, the optical density of the aggregated samples were measured at 600 nm. This method is very useful to detect aggregates with a hydrodynamic radius greater than the wavelength of light used.[24,41] The aggregation propensity

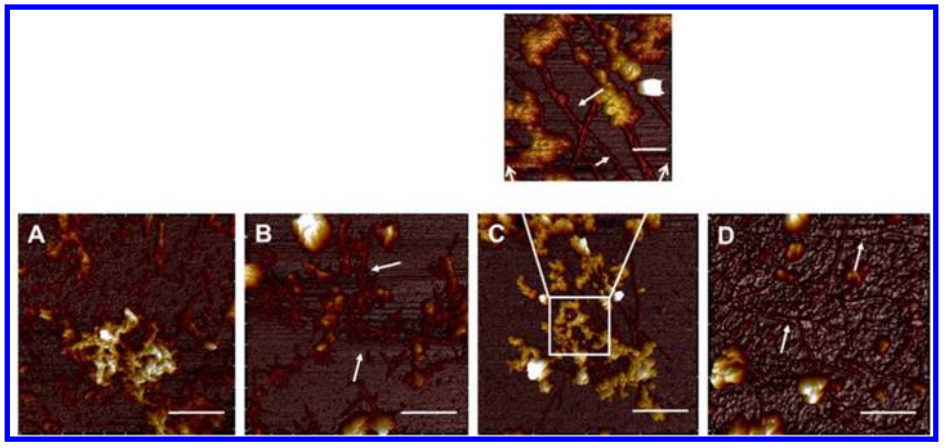

Figure 9. AFM Images of insulin aggregates after incubating with different timed seeds for 4 h. Insulin samples at 172 μM protein concentration were incubated for 4 h in the presence of seeds prepared by incubating for (A) 10 min (*nascent* seeds) (B) 30 min (*intermediate* seeds) (C) 1 h (*intermediate* seeds), and (D) 4 h (*intermediate* seeds). For panel A, B, C, and D the scale bar is 500 nm and the zoomed-in image in panel C is at 100 nm. Arrows indicate proto-fibrillar structures.

DOI: 10.1021/acs.jpcb.5b07221
J. Phys. Chem. B XXXX, XXX, XXX−XXX

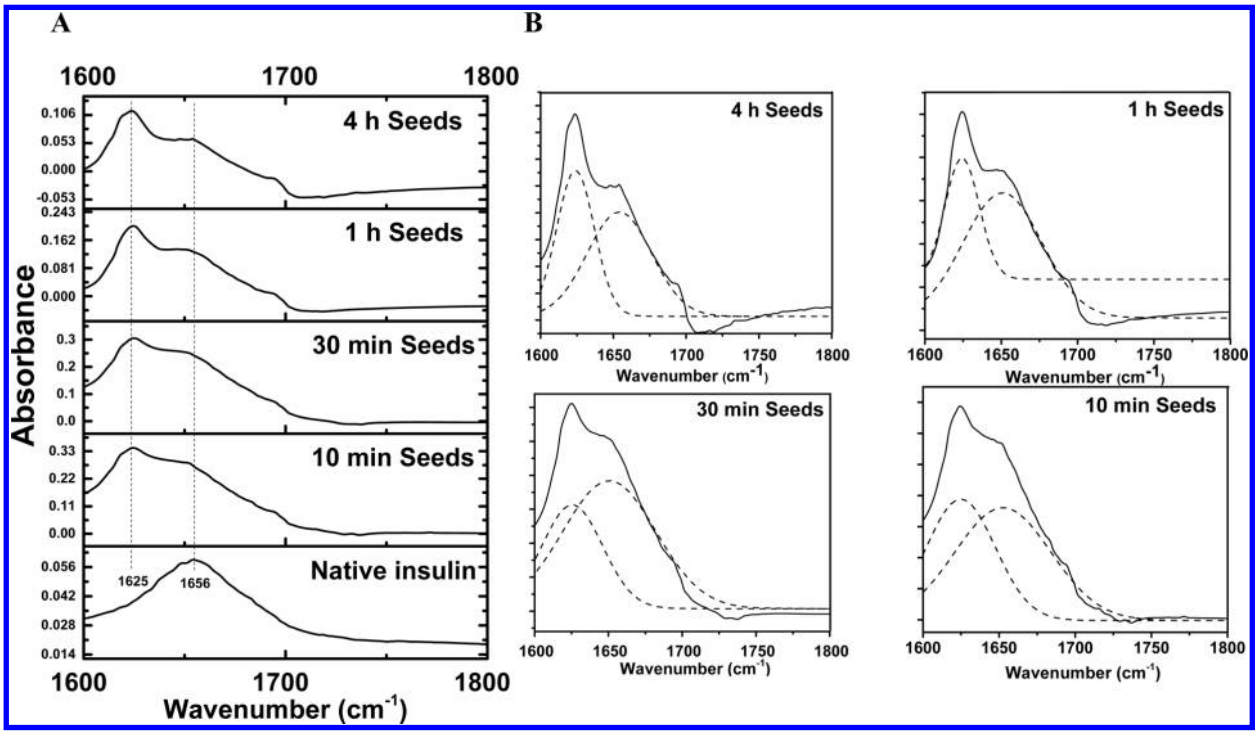

Figure 10. FT-IR Spectra for the amide I region of insulin aggregates. Aggregates were prepared by incubating 1 mg/mL insulin with 10 mM DTT for 10 min, 30 min, 1 h, and 4 h along with spectra of native protein. (A) Raw FT-IR spectra showing that amide bands are observed near 1656 and 1625 wavenumbers. (B) Raw FT-IR spectra (solid lines) and their component peaks (dotted lines) for the seeds.

was highest in the first 20 min, after which the process slowed down considerably. Proteins that were incubated for shorter time periods showed a very sharp increase in absorbance within the first 10 min, implying rapid initial aggregation (inset in Figure 3). This suggests increased instability and unfolding of insulin in presences of DTT that leads to misfolding and aggregation of the protein within 10 min of incubation. Controls similarly incubated in the absence of DTT did not exhibit any turbidity or increase in absorbance.

Insulin does not have any tryptophan residues therefore intrinsic fluorescence of insulin was measured by monitoring the exposure of tyrosine (Tyr) residues at 306 nm.[42,43] Decrease in fluorescence intensity at 306 nm (Figure 4) suggests exposure of Tyr residues to polar (aqueous) environment leading to fluorescence quenching as a consequence of protein unfolding.[44] Fluorescence intensity decreases rapidly in first 20 min followed by a gradual decrease up to 48 h, which is in line with the UV absorbance data. This suggests that insulin in the presence of disulfide reducing agent unfolds rapidly exposing the hydrophobic core (aromatic residues) followed by aggregation. This can be a direct result of catalytic amount of reducing agent promoting '*disulfide scrambling*' and drastically altering the protein stability.[21,25,26] The effect of 10 mM DTT on protein misfolding and hydrophobic exposure was measured using fluorescent dye ANS and its dimeric analogue bis-ANS. ANS is highly fluorescent and blue shifts (peak maximum shifts to 470 nm) upon binding to the hydrophobic core of the protein.[45] The dimeric analogue of ANS, bis-ANS shares similar properties to ANS but has a higher binding affinity for molten globule like structures of proteins (Figure 5). Both dyes exhibit similar trends with rapid increase in fluorescence intensity in the first h followed by high but steady fluorescence emission at longer incubation times. In presence of disulfide reduced insulin at 172 μM concentration, ANS shows rapid increase in fluorescence in the first few min of incubation that peaks and then steadies in 1 h (Figure 4A). The peak wavelength for ANS stays steady at ~470 nm for the length of incubation (Figure S4). The disulfide reduced insulin at 90 and 20 μM also showed emission spectra similar to that seen for 172 μM protein (Figure S5A, S5C). Interestingly, at these lower protein concentrations the peak wavelength for ANS that is initially around 500 nm shifts to ~470 nm in about 20 min and stays steady at ~470 nm even upon longer incubation (Figure S5B, S5D). This suggests that disulfide reduced insulin unfolds and the hydrophobic amino acid residues that are initially solvent exposed collapse and aggregate burying the hydrophobic residues (Figure S5). At protein concentration of 172 μM the unfolded protein burden is very high and it rapidly undergoes hydrophobic collapse aggregating with peak wavelength observed at ~470 nm. Controls (proteins with intact disulfide bonds) did not show change in fluorescence as a function of time. This is in line with other protein aggregation studies where exposure of hydrophobic amino acids is followed by collapse and burial of the hydrophobic core.[35,46−48]

ThT was used to investigate the nature of insulin aggregates. ThT showed very rapid increase in fluorescence in the first 1 h of incubation with disulfide reduced insulin followed by gradual increase in fluorescence for the rest of the length of incubation (Figure 6). This observed trend of fluorescence increase for ThT is similar to earlier protein aggregation studies suggesting amyloid formation.[27,49−51] The interaction between ThT molecules and amyloid β-sheets results in high fluorescent emission at 480 nm.[45] However, some other studies have shown that ThT dye can also interact with large amorphous aggregates by stacking in between the aggregates, leading to increased fluorescence.[52,53] Therefore, ThT fluorescence alone cannot accurately provide structural information about protein

DOI: 10.1021/acs.jpcb.5b07221
J. Phys. Chem. B XXXX, XXX, XXX−XXX

aggregates and needs further independent verification. We used SEM to image the aggregates and visualize the morphology of these aggregates. Electron microscope images show that the aggregates are amorphous in nature (Figure 6) that stay amorphous even upon longer incubation (Figure S7). Size of aggregates ranged between 100 and 200 nm, depending on the length of incubation (Figures 7, S6, S7).[30] Comparing the aggregates formed during the first 15 min (Figure 6A) with longer incubation time, the density of aggregates was seen to increase dramatically with time (Figure S6) but the nature of aggregates remained amorphous. As shown, large insulin aggregates were made of smaller units, suggesting a mechanism similar to '*chain polymerization*' (Figure S6). This implies that unfolded insulin monomer comes together to form multimers that in turn join together to form macromolecular aggregates. SEM image of fresh insulin with DTT (control sample, Figure S6B) shows very few aggregates that rapidly increases in size and number of aggregates in the first 15 min, after which the change is not as dramatic. This is in line with the observed data for unfolding, misfolding, and aggregation kinetics of insulin (Figures 3−6 and 8). Studies by several groups have suggested that amorphous aggregates are precursors of amyloid fibrils.[31,37,54,55] In order to test if disulfide-reduced insulin at physiological pH that are initially observed as amorphous aggregates turn into fibril; we imaged similarly incubated insulin (pH 7.2, 37 °C) samples after 6 months (Figure S7). We only observed amorphous aggregates even after such a long incubation time under the experimental conditions (Figure S7). These results are in line with other reports showing formation of amorphous aggregates even upon longer incubation.[31,56,57]

Salt has been shown to accelerate protein aggregation.[58,59] Effect of salt concentration was illustrated in the absence and presence of NaCl (150 or 300 mM) (Figures S1−S3). Aggregation kinetics showed trends that were similar for proteins with/without NaCl and the results were comparable to our earlier results (Figures 3−6), at all protein concentrations (Figures S1−S3). This suggests that insulin aggregation under reducing conditions is independent of ionic strength at pH 7.2. These results are in line with another study where chaotropic role of NaCl was absent in the process of insulin aggregation, both at acidic and at neutral pH.[11]

Insulin has been shown to aggregate at repeated injection sites of diabetic patients leading to a critical medical condition known as injection amyloidosis.[8] Many studies have shown that aggregation of proteins is propagated by a nucleation-dependent polymerization method where a "nucleus" is formed by assembly of monomers. Although, this process is thermodynamically and kinetically unfavorable, it decreases the energy barrier for aggregation, reducing the lag time and shifting the equilibrium toward unfolded state of the protein.[24,60] To understand how nucleation can impact aggregation of native insulin we prepared "*seeds*" by incubating insulin in the presence of 10 mM DTT for 10 min, 30 min to 4 h (30 min interval), and 5 to 12 h (1 h interval). Effect of seeding on native insulin aggregation was monitored by ThT fluorescence (Figure S14). The ThT fluorescence data for different timed *seeds* up to 4 h was fitted and analyzed by linear regression (Figure S13). The slope of the curves shows the kinetics of aggregation (Table S1). Aggregation kinetics of native insulin in the presence of 10 min *seeds* was maximum with a slope of 235.92 ± 4.86 (Table S1); followed by *seeds* made by incubating insulin for 30 min and 4 h. Aggregation of native insulin in the presence of *seeds* prepared by incubating protein for 5 h or longer (up to 12 h) had the slowest aggregation kinetics (Figure S13). Therefore, these seeds were grouped into *nascent* (10 min), *intermediate* (30 min to 4 h) and *mature* (5 to 12 h) *seeds* based on the difference in their aggregation kinetics (Table S1 and Figures S13 and S14).

The rate of aggregation increases continuously in the presence of *nascent* seeds at a concentration of 5% and 15% v/v (Figures S8 and S9). However, at a concentration of 45% (Figure S10), the aggregation rate is independent of "stage" of seeds (nascent, intermediate, or mature seeds) used to initiate aggregation. This maybe a result of saturation of the number of nucleation sites available for aggregation. This establishes the critical concentration of seeds necessary for proteins to aggregate *in vitro* and that still shows a difference in aggregation kinetics. In summary, *nascent* seeds had the shortest lag time and fastest aggregation kinetics. This suggests that *nascent* seeds of insulin have high number of soluble misfolded proteins with exposed hydrophobic surface providing very high number of nucleation sites for native insulin to bind and aggregate compared to seeds prepared by longer incubation. The kinetics of aggregation was also observed to linearly depend on the seeding concentration in the presence of *nascent* seeds (Figure 8). This suggests that at higher seed concentration (e.g., 15% seed v/v) the number of available nucleation sites for seeds are more compared to seed concentration of 5% v/v and hence higher aggregation rate observed at higher concentration (Figure 8). This is in line with another study that suggests partially folded protein intermediates promote aggregation and not the mature aggregates.[35]

Morphology of the aggregates formed as a result of seeding were characterized by atomic force microscopy (Figures 9, S11, and S12). The aggregates formed by native insulin incubated with *nascent* or *intermediate* seeds increased in size from 10 to 400 nm (Figure S11). Stiffness of aggregates as measured by Young's modulus ranged between 4 ± 0.6 to 6 ± 0.2 GPa for the aggregates formed by *nascent* and *intermediate* seeds, which is comparable to values reported in literature.[61−64] These values suggest that the aggregates are relatively rigid and the high tensile strength of these aggregates maybe a result of strong hydrogen bonding as well as hydrophobic interactions contributing to the mechanical stiffness of the structure.[64,65] Interestingly, native insulin when incubated with *intermediate* seeds formed fibrils (Figure 8B, 8C) that converted to amorphous aggregates upon longer incubation (24 h or more) (Figure S12). The secondary structure of *nascent* and *intermediate* seeds along with native insulin (control) was investigated using FT-IR[66,67] to understand the morphological diversity of the seeds (Figure 10). A peak at 1656 cm^{-1} was observed for native insulin that is characteristic of α-helical proteins.[68−71] All the *seeds* show a peak at 1625 cm^{-1} that is characteristic of β-sheet structure. The raw spectra were deconvoluted and fitted using Gaussian function to obtain the major component peaks. Area under the deconvoluted peaks were integrated to calculate the percent contribution from α-helical or β-sheet structures, for each seeds. The α-helical content decreased with increase in incubation time. *Nascent seeds* (10 min) had nearly 63% of α-helical and 37% of β-sheet structures (Figure 10). This ratio changed to ∼50% α-helical and ∼50% β-sheet for *intermediate seeds* (4 h). This suggests that the *nascent* seeds have significant native structure (α-helix) that can contribute to native insulin aggregation in a nucleation dependent manner. In *nascent seeds* the α-helical

DOI: 10.1021/acs.jpcb.5b07221
J. Phys. Chem. B XXXX, XXX, XXX−XXX

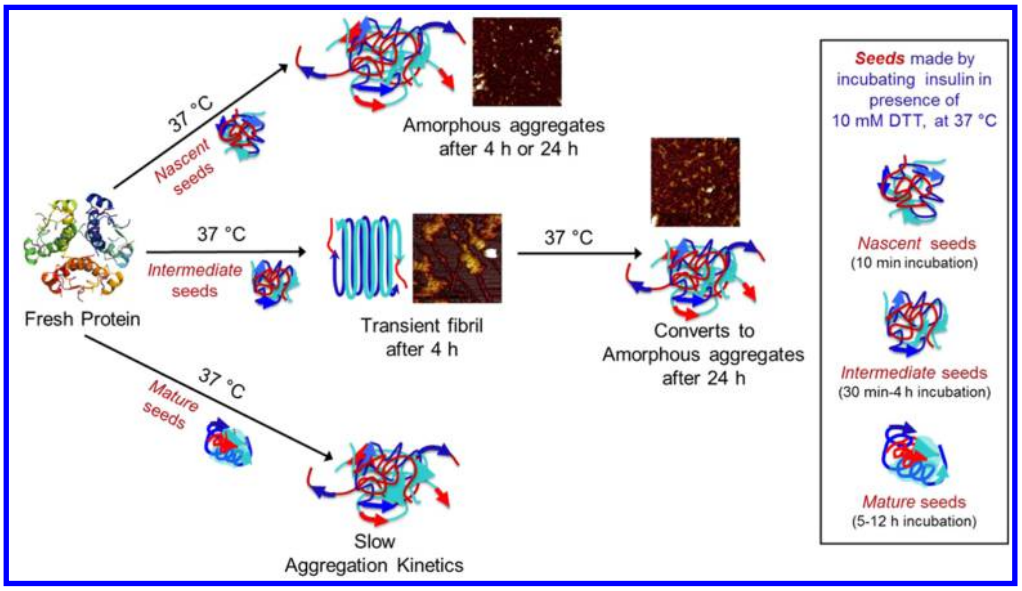

Figure 11. Plausible aggregation mechanism model based on insulin aggregation in the presence of different timed seeds. *Nascent* seeds promote rapid amorphous aggregate formation; *intermediate* seeds lead to formation of fibrillar structure in 4 h that converts to amorphous upon longer incubation of 24 h. Aggregation in the presence of *mature* seeds is very slow when compared to *nascent* and *intermediate* seed kinetics.

structure acts as the site of nucleation for native insulin and the β-sheet component propagates the aggregation process in a template-dependent manner. *Intermediate seeds* (30 min to 4 h) could also promote aggregation of native insulin due to the presence of significant α-helical structure (50% to 60%) present in them. AFM images of *intermediate* seeds incubated with native protein show formation of protofibrillar to fibrillar structures. This observation is complemented by FTIR data wherein increase in β-sheet structure is observed for both 1 and 4 h seeds. Kinetic data shows that 1 h seed is most efficient among *intermediate* seeds, in aggregating native insulin, which suggests that protofibrils are more efficient than fibrils in aggregating native insulin (Table S1 and Figure 10). Conversion of fibrils to amorphous aggregates within 24 h of incubation under our experimental conditions shows the transient nature of these aggregates (Figure 11). This is in line with amorphous aggregates observed for disulfide-reduced insulin incubated at 37 °C for 6 months in this study. Overall, this study and an earlier study shows that proteins under conditions that are reducing and close to physiological favor formation of amorphous aggregates.[57]

CONCLUSION

In summary, this study measures the aggregation kinetics and characterizes the nature of aggregates of insulin formed under disulfide reducing conditions at pH 7.2 and 37 °C. The results show that insulin aggregates rapidly under these conditions and forms amorphous aggregates that stay amorphous even upon incubation for six months. *Seeds* affect native insulin aggregation kinetics, with *nascent* seeds showing the fastest aggregation kinetics. Interestingly, incubation of native insulin with *intermediate* seeds for shorter period (4 h) results in fibril formation that converts to amorphous upon longer incubation (24 h). These results suggests that insulin favors amorphous aggregate formation under disulfide reducing conditions at physiological pH and temperature.

ASSOCIATED CONTENT

Supporting Information

The Supporting Information is available free of charge on the ACS Publications website at DOI: 10.1021/acs.jpcb.5b07221.

Figures S1−S14 and Table S1, including effect of electrostatic interactions on insulin misfolding and aggregation monitored by intrinsic fluorescence, bis-ANS, and ThT fluorescence, insulin aggregation monitored by ANS fluorescence peak intensity and wavelength shift as a function of time, scanning electron microscope images of insulin aggregates for different times including samples incubated for 6 months. effect of seeding on native insulin aggregation monitored by ThT fluorescence, AFM images of aggregated insulin, and aggregation kinetics analysis (PDF)

AUTHOR INFORMATION

Corresponding Author

*(A.T.) Telephone: (906) 487-1840. Fax: (906) 487-2061. E-mail: tiwari@mtu.edu.

Author Contributions

A.T., C.D., and M.Y. designed the experiments. C.D. and M.Y. performed the experiments. A.T., C.D., and M.Y. analyzed the data. A.T. and C.D. wrote the paper. AFM experiments were designed by A.T., R.S.-Y., C.D., and F.L. C.D. and F.L. performed the experiments and R.S.-Y., C.D., and F.L. analyzed the data. All authors commented on the manuscript. All authors have given approval to the final version of the manuscript

Notes

The authors declare no competing financial interests.

ACKNOWLEDGMENTS

This work was supported by MTU new faculty startup funds and research excellence funds to AT. RS-Y acknowledges financial support from the National Science Foundation (Award No. DMR-1100806) for the atomic force microscopy-related tasks.

DOI: 10.1021/acs.jpcb.5b07221
J. Phys. Chem. B XXXX, XXX, XXX−XXX

REFERENCES

(1) Centers for Disease Control and Prevention. *National Diabetes Statistics Report: Estimates of Diabetes and Its Burden in the United States*; U.S. Department of Health and Human Services: Atlanta, GA, 2014.

(2) Gasparini, L.; Netzer, W. J.; Greengard, P.; Xu, H. X. Does Insulin Dysfunction Play a Role in Alzheimer's Disease? *Trends Pharmacol. Sci.* **2002**, *23*, 288−293.

(3) Brems, D. N.; Brown, P. L.; Bryant, C.; Chance, R. E.; Green, L. K.; Long, H. B.; Miller, A. A.; Millican, R.; Shields, J. E.; Frank, B. H. Improved Insulin Stability Through Amino-Acid Substitution. *Protein Eng., Des. Sel.* **1992**, *5*, 519−525.

(4) Wang, W. Protein Aggregation and its Inhibition in Biopharmaceutics. *Int. J. Pharm.* **2005**, *289*, 1−30.

(5) Givol, D.; Lorenzo, F. D.; Goldberger, R. F.; Anfinsen, C. B. Disulfide Interchange and the Three-Dimensional Structure of Proteins. *Proc. Natl. Acad. Sci. U. S. A.* **1965**, *53*, 676−684.

(6) Morris, H. R.; Pucci, P.; Panico, M.; Marino, G. Protein Folding/Refolding Analysis by Mass Spectrometry. Scrambling of Disulphide Bridges in Insulin. *Biochem. J.* **1990**, *268*, 803−806.

(7) Gerweck, L. E.; Seetharaman, K. Cellular pH Gradient in Tumor Versus Normal Tissue: Potential Exploitation for the Treatment of Cancer. *Cancer Res.* **1996**, *56*, 1194−1198.

(8) Dische, F. E.; Wernstedt, C.; Westermark, G. T.; Westermark, P.; Pepys, M. B.; Rennie, J. A.; Gilbey, S. G.; Watkins, P. J. Insulin as an Amyloid-Fibril Protein at Sites of Repeated Insulin Injections in a Diabetic Patient. *Diabetologia* **1988**, *31*, 158−161.

(9) Ahmad, A.; Millett, I. S.; Doniach, S.; Uversky, V. N.; Fink, A. L. Stimulation of Insulin Fibrillation by Urea-Induced Intermediates. *J. Biol. Chem.* **2004**, *279*, 14999−15013.

(10) Jiang, C. T.; Chang, J. Y. Unfolding and Breakdown of Insulin in the Presence of Endogenous Thiols. *FEBS Lett.* **2005**, *579*, 3927−3931.

(11) Arora, A.; Ha, C.; Park, C. B. Insulin Amyloid Fibrillation at Above 100 Degrees C: New Insights into Protein Folding Under Extreme Temperatures. *Protein Sci.* **2004**, *13*, 2429−2436.

(12) Ahmad, A.; Millett, I. S.; Doniach, S.; Uversky, V. N.; Fink, A. L. Partially Folded Intermediates in Insulin Fibrillation. *Biochemistry* **2003**, *42*, 11404−11416.

(13) Sluzky, V.; Tamada, J. A.; Klibanov, A. M.; Langer, R. Kinetics of Insulin Aggregation in Aqueous-Solutions upon Agitation in the Presence of Hydrophobic Surface. *Proc. Natl. Acad. Sci. U. S. A.* **1991**, *88*, 9377−9381.

(14) Brange, J.; Andersen, S.; Laursen, E. D.; Meyn, G.; Rasmussen, E. Towards Understanding Insulin Fibrillation. *J. Pharm. Sci.* **1997**, *86*, 517−525.

(15) Hua, Q. X. Insulin: a Small Protein with a Long Journey. *Protein Cell* **2010**, *1*, 537−551.

(16) Nielsen, L.; Khurana, R.; Coats, A.; Frokjaer, S.; Brange, J.; Vyas, S.; Uversky, V. N.; Fink, A. L. Effect of Environmental Factors on the Kinetics of Insulin Fibril Formation: Elucidation of the Molecular Mechanism. *Biochemistry* **2001**, *40*, 6036−6046.

(17) Westermark, P.; Andersson, A.; Westermark, G. T. Islet Amyloid Polypeptide, Islet Amyloid, and Diabetes Mellitus. *Physiol. Rev.* **2011**, *91*, 795−826.

(18) Bouchard, M.; Zurdo, J.; Nettleton, E. J.; Dobson, C. M.; Robinson, C. V. Formation of Insulin Amyloid Fibrils Followed by FTIR Simultaneously with CD and Electron Microscopy. *Protein Sci.* **2000**, *9*, 1960−1967.

(19) Dzwolak, W.; Ravindra, R.; Lendermann, J.; Winter, R. Aggregation of Bovine Insulin Probed by DSC/PPC Calorimetry and FTIR Spectroscopy. *Biochemistry* **2003**, *42*, 11347−11355.

(20) Hong, D. P.; Ahmad, A.; Fink, A. L. Fibrillation of Human Insulin A and B Chains. *Biochemistry* **2006**, *45*, 9342−9353.

(21) Hua, Q. X.; Weiss, M. A. Mechanism of Insulin Fibrillation - the Structure of Insulin under Amyloidogenic Conditions Resembles a Protein-Folding Intermediate. *J. Biol. Chem.* **2004**, *279*, 21449−21460.

(22) Grudzielanek, S.; Jansen, R.; Winter, R. Solvational Tuning of the Unfolding, Aggregation and Amyloidogenesis of Insulin. *J. Mol. Biol.* **2005**, *351*, 879−894.

(23) Dzwolak, W.; Smirnovas, V.; Jansen, R.; Winter, R. Insulin Forms Amyloid in a Strain-Dependent Manner: an FT-IR Spectroscopic Study. *Protein Sci.* **2004**, *13*, 1927−1952.

(24) Jarrett, J. T.; Lansbury, P. T., Jr. Seeding "One-Dimensional Crystallization" of Amyloid: A Pathogenic Mechanism in Alzheimer's Disease and Scrapie? *Cell* **1993**, *73*, 1055−1058.

(25) Toichi, K.; Yamanaka, K.; Furukawa, Y. Disulfide Scrambling Describes the Oligomer Formation of Superoxide Dismutase (SOD1) Proteins in the Familial Form of Amyotrophic Lateral Sclerosis. *J. Biol. Chem.* **2013**, *288*, 4970−4980.

(26) Trivedi, M. V.; Laurence, J. S.; Siahaan, T. J. The Role of Thiols and Disulfides in Protein Chemical and Physical Stability. *Curr. Protein Pept. Sci.* **2009**, *10*, 614−625.

(27) Li, Y.; Gong, H.; Sun, Y.; Yan, J.; Cheng, B. A.; Zhang, X.; Huang, J.; Yu, M.; Guo, Y.; Zheng, L.; Huang, K. Dissecting the Role of Disulfide Bonds on the Amyloid Formation of Insulin. *Biochem. Biophys. Res. Commun.* **2012**, *423*, 373−378.

(28) Huang, K.; Maiti, N. C.; Phillips, N. B.; Carey, P. R.; Weiss, M. A. Structure-Specific Effects of Protein Topology on Cross-Beta Assembly: Studies of Insulin Fibrillation. *Biochemistry* **2006**, *45*, 10278−10293.

(29) Chang, X.; Jørgensen, A. M.; Bardrum, P.; Led, J. J. Solution Structures of the R6 Human Insulin Hexamer. *Biochemistry* **1997**, *36*, 9409−9422.

(30) Krebs, M. R. H.; Devlin, G. L.; Donald, A. M. Protein Particulates: Another Generic Form of Protein Aggregation? *Biophys. J.* **2007**, *92*, 1336−1342.

(31) Stefani, M.; Rigacci, S. Protein Folding and Aggregation into Amyloid: The Interference by Natural Phenolic Compounds. *Int. J. Mol. Sci.* **2013**, *14* (6), 12411−12457.

(32) Westermark, P. Aspects on Human Amyloid Forms and their Fibril Polypeptides. *FEBS J.* **2005**, *272*, 5942−5949.

(33) Khurana, R.; Coleman, C.; Ionescu-Zanetti, C.; Carter, S. A.; Krishna, V.; Grover, R. K.; Roy, R.; Singh, S. Mechanism of Thioflavin T Binding to Amyloid Fibrils. *J. Struct. Biol.* **2005**, *151*, 229−238.

(34) Ahmad, A.; Uversky, V. N.; Hong, D.; Fink, A. L. Early Events in the Fibrillation of Monomeric Insulin. *J. Biol. Chem.* **2005**, *280*, 42669−42675.

(35) Nielsen, L.; Frokjaer, S.; Brange, J.; Uversky, V. N.; Fink, A. L. Probing the Mechanism of Insulin Fibril Formation with Insulin Mutants. *Biochemistry* **2001**, *40*, 8397−8409.

(36) Groenning, M.; Frokjaer, S.; Vestergaard, B. Formation Mechanism of Insulin Fibrils and Structural Aspects of the Insulin Fibrillation Process. *Curr. Protein Pept. Sci.* **2009**, *10*, 509−528.

(37) Fink, A. L. Protein Aggregation: Folding Aggregates, Inclusion Bodies and Amyloid. *Folding Des.* **1998**, *3*, R9−R23.

(38) Yoshimura, Y.; Lin, Y. X.; Yagi, H.; Lee, Y. H.; Kitayama, H.; Sakurai, K.; So, M.; Ogi, H.; Naiki, H.; Goto, Y. Distinguishing Crystal-Like Amyloid Fibrils and Glass-Like Amorphous Aggregates from their Kinetics of Formation. *Proc. Natl. Acad. Sci. U. S. A.* **2012**, *109*, 14446−14451.

(39) Tiwari, A.; Hayward, L. J. Familial Amyotrophic Lateral Sclerosis Mutants of Copper/Zinc Superoxide Dismutase are Susceptible to Disulfide Reduction. *J. Biol. Chem.* **2003**, *278*, 5984−5992.

(40) Lee, J. Y.; Hirose, M. Partially Folded State of the Disulfide-reduced Form of Human Serum Albumin as an Intermediate for Reversible Denaturation. *J. Bio. Chem.* **1992**, *267*, 14753−14758.

(41) Creighton, T. E. Disulphide Bonds and Proteins Stability. *BioEssays* **1988**, *8*, 57−63.

(42) Jarrett, J. T.; Lansbury, P. T., Jr. Amyloid Fibril Formation Requires a Chemically Discriminating Nucleating Event: Studies of an Amyloidogenic Sequence from the Bacterial Protein OsmB. *Biochemistry* **1992**, *31* (49), 12345−12352.

(43) Vincentelli, R.; Canaan, S.; Campanacci, V.; Valencia, C.; Maurin, D.; Frassinetti, F.; Scappucini-Calvo, L.; Bourne, Y.;

DOI: 10.1021/acs.jpcb.5b07221
J. Phys. Chem. B XXXX, XXX, XXX−XXX

Cambillau, C.; Bignon, C. High-Throughput Automated Refolding Screening of Inclusion Bodies. *Protein Sci.* **2004**, *13*, 2782−2792.
(44) Cromwell, M. E. M.; Hilario, E.; Jacobson, F. *Protein Aggregation and Bioprocessing*. Paper Presented at the Proceedings of the 2005 AAPS Biotec Open Forum on Aggregation of Protein Therapeutics. San Francisco, CA.
(45) Vivian, J. T.; Callis, P. R. Mechanisms of Tryptophan Fluorescence Shifts in Proteins. *Biophys. J.* **2001**, *80*, 2093−2109.
(46) Hawe, A.; Sutter, M.; Jiskoot, W. Extrinsic Fluorescent Dyes as Tools for Protein Characterization. *Pharm. Res.* **2008**, *25*, 1487−1499.
(47) Pawar, A. P.; Dubay, K. F.; Zurdo, J.; Chiti, F.; Vendruscolo, M.; Dobson, C. M. Prediction of "Aggregation-Prone" and "Aggregation-Susceptible" Regions in Proteins Associated with Neurodegenerative Diseases. *J. Mol. Biol.* **2005**, *350*, 379−392.
(48) Dobson, C. M. Protein Folding and Misfolding. *Nature* **2003**, *426*, 884−890.
(49) Ali, V.; Prakash, K.; Kulkarni, S.; Ahmad, A.; Madhusudan, K. P.; Bhakuni, V. 8-Anilino-1-naphthalene Sulfonic Acid (ANS) Induces Folding of Acid Unfolded Cytochrome C to Molten Globule State as a Result of Electrostatic Interactions. *Biochemistry* **1999**, *38*, 13635−13642.
(50) Makin, O. M.; Serpell, L. C. Structure of Amyloid Fibrils. *FEBS J.* **2005**, *272*, 5950−5961.
(51) Krebs, M. R. H.; Bromley, E. H.; Donald, A. M. The Binding of Thioflavin-T to Amyloid Fibrils: Localisation and Implications. *J. Struct. Biol.* **2005**, *149*, 30−37.
(52) Groenning, M.; Olsen, L.; Van de Weert, M.; Flink, J. M.; Frokjaer, S.; Jørgensen, F. S. Study on the Binding of Thioflavin T to Beta-Sheet-Rich and Non-Beta-Sheet Cavities. *J. Struct. Biol.* **2007**, *158*, 358−369.
(53) Ellis, R. J.; Pinheiro, T. J. Medicine: Danger – Misfolding proteins. *Nature* **2002**, *416*, 483−484.
(54) Chiti, F.; Dobson, C. M. Protein Misfolding, Functional Amyloid, and Human Disease. *Annu. Rev. Biochem.* **2006**, *75*, 333−366.
(55) Kopito, R. R. Aggresomes, Inclusion Bodies and Protein Aggregation. *Trends Cell Biol.* **2000**, *10*, 524−530.
(56) Stefani, M. Biochemical and Biophysical Features of both Oligomer/Fibril and Cell Membrane in Amyloid Cytotoxicity. *FEBS J.* **2010**, *277*, 4602−4613.
(57) Yang, M.; Dutta, C.; Tiwari, A. Disulfide Bond Scrambling Promotes Amorphous Aggregates in Lysozyme and Bovine Serum Albumin. *J. Phys. Chem. B* **2015**, *119* (10), 3969−81.
(58) Muzaffar, M.; Ahmad, A. The Mechanism of Enhanced Insulin Amyloid Fibril Formation by NaCl Is Better Explained by a Conformational Change Model. *PLoS One* **2011**, *6* (11), e27906.
(59) Chi, E. Y.; Krishnan, S.; Kendrick, B. S.; Chang, B. S.; Carpenter, J. F.; Randolph, T. W. Roles of Conformational Stability and Colloidal Stability in the Aggregation of Recombinant Human Granulocyte Colony-Stimulating Factor. *Protein Sci.* **2003**, *12*, 903−913.
(60) Harper, J. D.; Lansbury, P. T., Jr. Models of Amyloid Seeding in Alzheimer's Disease and Scrapie: Mechanistic Truths and Physiological Consequences of the Time-Dependent Solubility of Amyloid Proteins. *Annu. Rev. Biochem.* **1997**, *66*, 385−407.
(61) Adamcik, J.; Lara, C.; Usov, I.; Jeong, J. S.; Ruggeri, F. S.; Dietler, G.; Lashuel, H. A.; Hamley, I. W.; Mezzenga, R. Measurement of Intrinsic Properties of Amyloid Fibrils by Peak Force QNM Method. *Nanoscale* **2012**, *4*, 4426−4429.
(62) Adamcik, J.; Berquand, A.; Mezzenga, R. Single-step direct measurement of amyloid fibrils stiffness by peak force quantitative nanomechanical atomic force microscopy. *Appl. Phys. Lett.* **2011**, *98*, 193701.
(63) Adamcik, J.; Mezzenga, R. Study of amyloid fibrils via atomic force microscopy. *Curr. Opin. Colloid Interface Sci.* **2012**, *17* (6), 369−376.
(64) Smith, J. F.; Knowles, T. P.; Dobson, C. M.; MacPhee, C. E.; Welland, M. E. Characterization of nanoscale properties of individual amyloid fibrils. *Proc. Natl. Acad. Sci. U. S. A.* **2006**, *103* (43), 15806−15811.
(65) Knowles, T. P.; Fitzpatrick, A. W.; Meehan, S.; Mott, H. R.; Vendruscolo, M.; Dobson, C. M.; Welland, M. E. Role of intermolecular forces in defining material properties of protein nanofibrils. *Science* **2007**, *318*, 1900−1903.
(66) Srivastava, A.; Arya, P.; Goel, S.; Kundu, B.; Mishra, P.; Fnu, A. Gelsolin Amyloidogenesis Is Effectively Modulated by Curcumin and Emetine Conjugated PLGA Nanoparticles. *PLoS One* **2015**, *10* (5), e0127011.
(67) Arya, P.; Srivastava, A.; Vasaikar, S. V.; Mukherjee, G.; Mishra, P.; Kundu, B. Selective Interception of Gelsolin Amyloidogenic Stretch Results in Conformationally Distinct Aggregates with Reduced Toxicity. *ACS Chem. Neurosci.* **2014**, *5*, 982−992.
(68) Shivu, B.; Seshadri, S.; Li, J.; Oberg, K. A.; Uversky, V. N.; Fink, A. L. Distinct β-sheet Structure in Protein Aggregates Determined by ATR-FTIR Spectroscopy. *Biochemistry* **2013**, *52*, 5176−5183.
(69) Zako, T.; Sakono, M.; Hashimoto, N.; Ihara, M.; Maeda, M. Bovine Insulin filaments Induced by Reducing Disulfide Bonds Show a Different Morphology, Secondary Structure, and Cell toxicity from Intact Insulin Amyloid Fibrils. *Biophys. J.* **2009**, *96*, 3331−3340.
(70) Kong, J.; Yu, S. Fourier Transform Infrared Spectroscopic Analysis of Protein Secondary Structures. *Acta Biochim. Biophys. Sin.* **2007**, *39* (8), 549−559.
(71) Amenabar, I.; Poly, S.; Nuansing, W.; Hubrich, E. H.; Govyadinov, A. A.; Huth, F.; Krutokhvostov, R.; Zhang, L.; Knez, M.; Heberle, J.; Bittner, A. M.; Hillenbrand, R. Structural Analysis of Mapping of Individual Protein Complexes by Infrared Nanospectroscopy. *Nat. Commun.* **2013**, *4*, 2890.

DOI: 10.1021/acs.jpcb.5b07221
J. Phys. Chem. B XXXX, XXX, XXX−XXX